Investigating Piecewise Linear Energy Storage Models for Optimization in Power Systems

Lysandros Tziovani, Lenos Hadjidemetriou, Stelios Timotheou
KIOS Research and Innovation Center of Excellence and Department of Electrical and Computer Engineering
University of Cyprus
Nicosia, Cyprus
{ltziov01, lhadji02, stimo}@ucy.ac.cy

***Abstract*—Energy storage systems (ESSs) are increasingly used in power system optimization by deriving different ESS mathematical models. The most widely-used model is the piecewise linear ESS model which utilizes non-convex constraints to represent the ESS power losses, resulting in challenging optimization problems. To reduce the problem complexity, convex relaxation models are often derived but may compromise the solution quality of the underlying problems. This work investigates the exact and relaxed versions of three different mathematical representations of the piecewise linear ESS model, in terms of their solution quality and execution efficiency. Towards this direction, the three ESS models are incorporated into the unit commitment problem which often violates the ESS relaxation exactness under ramping constraints. Simulation results present (a) the execution times of the exact and relaxed ESS models and (b) the optimality gap of the relaxed models when the relaxation exactness is violated.**

***Index Terms*—Convex relaxation, energy storage models, optimization, unit commitment.**

I. Introduction

ENERGY Storage Systems (ESSs) is an emerging technology that can be used to compensate the negative effects imposed by the uncontrollable generation of renewable energy sources (RES) into the power systems. In general, ESSs can provide several functionalities in the electricity sector including the provision of grid services and the management of energy resources for electricity cost reduction [1], [2]. Since these ESSs functionalities allow an increased and effective RES integration, the total energy storage capacity is expected to rapidly grow according to the European Union target to achieve climate-neutrality by 2050 [3].

Different mathematical models have been derived to represent ESSs in power system optimization problems, e.g., the piecewise linear and quadratic models [4]. These models uses non-convex constraints to represent the ESS power losses, resulting in non-convex optimization problems which are hard to solve. To reduce the problem complexity, relaxed ESS models are often derived by relaxing the non-convex constraints. This work considers three different equivalent mathematical representations of the widely-used piecewise linear model [4]. The first model deals with the non-convex equality constraints, where the ESS power losses are proportional to the absolute value of the charging/discharging power, by relaxing them to convex inequality constraints [4], [5]. The second model represents the charging/discharging power using two separable variables, eliminating the non-convex power losses constraint, but non-convex complementarity constraints are introduced to avoid simultaneous charging and discharging. Removing the complementarity constraints yields the second relaxed model [6]–[8]. The third model reformulates the complementarity constraints using binary variables and then relaxing them to take continuous values [9]. The relaxed ESS models can be used in power system applications that require fast solutions, e.g, using model predictive control, generating the optimal solution when the ESSs relaxation exactness is satisfied. However, infeasible solutions are generated when the relaxation exactness is violated.

The relaxed ESS models have been used to formulate convex optimization problems, which can be fast and reliably solved, to manage the ESSs charging/discharging power in active distribution grids [5], [6] and transmission networks [10]. Furthermore, the relaxed ESS models have been utilized in Unit Commitment (UC) formulations [11], [12], which are non-convex mixed-integer optimization problems, to reduce their computational complexity by decreasing the number of binary variables. The relaxation exactness is shown to hold in [6], [11] under some sufficient conditions; however, the ESSs relaxation can be non-exact in other formulations [10], [12].

This work presents the exact and relaxed versions of three ESS models derived from the widely-used piecewise linear model. The ESS models are integrated in a UC formulation which often violates the ESS relaxation exactness under ramping constraints of the conventional generating units. The contributions of this work regards the investigation of the exact and relaxed versions of three ESS models aiming to: (a) elaborate on the relaxation tightness, (b) examine their performance, in terms of execution time and solution accuracy, in the context of the UC problem, and (c) provide practical usage recommendations.

The rest of the paper is organized as follows. Section II states the problem and Section III describes the ESS models. The UC problem is formulated in Section IV and simulation results are shown in Section V. Conclusions are given in Section VI.

This work was supported in part by the European Union's Horizon 2020 Research and Innovation Programme under grant agreement No 957739 (OneNet) and 101075747 (TRANSIT); and in part by the European Union's Horizon 2020 research and innovation programme under grant agreement No 739551 (KIOS CoE - TEAMING) and from the Republic of Cyprus through the Deputy Ministry of Research, Innovation and Digital Policy.

II. Problem Statement

The generic ESS model that is incorporated in optimization problems is stated as

$$C_{t+1,k} = C_{t,k} + \Delta T(-P^S_{t,k} - P^L_{t,k}), \quad \forall t \in \mathcal{T}, k \in \mathcal{K}, \quad (1a)$$
$$C_{0,k} = I_k, \quad \underline{C}_k \leq C_{t,k} \leq \overline{C}_k, \quad \forall t \in \mathcal{T}, k \in \mathcal{K}, \quad (1b)$$
$$-\overline{P}^c_{t,k} \leq P^S_{t,k} \leq \overline{P}^d_{t,k}, \quad \forall t \in \mathcal{T}, k \in \mathcal{K}, \quad (1c)$$

where $\mathcal{T} = \{1, ..., T\}$ denotes the considered time horizon and ΔT the time-slot length in hours; $\mathcal{K} = \{1, ..., K\}$ denotes the number of ESSs. Variables $C_{t,k}$, $P^S_{t,k}$ and $P^L_{t,k}$ denote the ESS state-of-charge (SoC) in MWh, discharging ($P^S_{t,k} \geq 0$) and charging ($P^S_{t,k} < 0$) power in MW, and power losses in MW, respectively. Constraint (1a) describes the variation of the ESS SoC over time based on the charging/discharging power and power losses. Constraints (1b) and (1c) provide limits on the minimum and maximum SoC, $\underline{C}_k$ and $\overline{C}_k$, and discharging and charging power, $\overline{P}^d_{t,k}$ and $\overline{P}^c_{t,k}$, respectively, where I_k denotes the initial SoC.

Different ESS models are derived in the literature based on various functions that represent the ESS power losses in (1a), e.g., the piecewise linear and quadratic models [4]. The most widely-used model is the piecewise linear model given by

$$P^L_{t,k} = e|P^S_{t,k}|, \quad \forall t \in \mathcal{T}, k \in \mathcal{K}, \quad (2)$$

where e is a power losses coefficient. The absolute value in (2) is used to avoid negative losses when $P^S_{t,k} < 0$; therefore, the power losses are represented by two piecewise linear segments.

The incorporation of the ESS model (1a)-(2) in optimization formulations results in non-convex optimization problems, which are hard to solve, because the constraint (2) is non-convex. To reduce the problem complexity, the non-convex constraint (2) can be relaxed to the convex constraint

$$P^L_{t,k} \geq e|P^S_{t,k}|, \quad \forall t \in \mathcal{T}, k \in \mathcal{K}. \quad (3)$$

The solution of an optimization problem with the relaxed ESS model (1a)-(1c), (3) is optimal when the relaxation is exact i.e., the equality is attained in constraint (3); otherwise, the solution is infeasible. Specifically, increased ESS power losses are presented in the optimization problem when the relaxation is not exact, denoting that more energy is wasted than prescribed by the losses function. This work investigates three exact and relaxed ESS models derived from the piecewise-linear model in (2). Next, the ESS models are presented.

III. Piecewise Linear Energy Storage Models

This section provides the exact and relaxed formulation of three literature-based ESS models, derived from the widely-used piecewise-linear model in (2), and presents the feasible region of their ESS power losses.

A. Exact ESS Models

1) Exact Model E_1: The first exact model [5] reformulates the power losses function in (2) by defining the discharging and charging power losses

$$P^{L,d}_{t,k} = e^d_k P^S_{t,k}, \quad P^{L,c}_{t,k} = (-e^c_k) P^S_{t,k} \quad \forall t \in \mathcal{T}, k \in \mathcal{K}, \quad (4)$$

where e^d_k and e^c_k denote the positive discharging and charging losses coefficients. Note that $P^{L,d}_{t,k} \geq 0$ and $P^{L,c}_{t,k} \leq 0$ when $P^S_{t,k} \geq 0$ (discharging), while $P^{L,d}_{t,k} < 0$ and $P^{L,c}_{t,k} \geq 0$ when $P^S_{t,k} \leq 0$ (charging). Therefore, the power losses are defined as the maximum between $P^{L,d}_{t,k}$ and $P^{L,c}_{t,k}$, given by

$$P^L_{t,k} = \max(P^{L,d}_{t,k}, P^{L,c}_{t,k}), \quad \forall t \in \mathcal{T}, k \in \mathcal{K}. \quad (5)$$

The non-convex constraint (5) can equivalently be reformulated using binary variables, $b_{t,k} \in \{0, 1\}$, and the big-M method, yielding the model formulation, for all $t \in \mathcal{T}$, $k \in \mathcal{K}$

$$\text{Constraints (1a)} - \text{(1b)}, \quad (6a)$$
$$-\overline{P}^c_{t,k}(1 - b_{t,k}) \leq P^S_{t,k} \leq b_{t,k}\overline{P}^d_{t,k}, \quad (6b)$$
$$e^d_k P^S_{t,k} \leq P^L_{t,k} \leq e^d_k P^S_{t,k} + M^a_k(1 - b_{t,k}), \quad (6c)$$
$$-e^c_k P^S_{t,k} \leq P^L_{t,k} \leq -e^c_k P^S_{t,k} + M^b_k b_{t,k}, \quad (6d)$$

where constants $M^a_k \geq (e^c_k + e^d_k)\overline{P}^c_{t,k}$ and $M^b_k \geq (e^c_k + e^d_k)\overline{P}^d_{t,k}$. Constraint (6b) ensures that $b_{t,k} = 1$ when $P^S_{t,k} \geq 0$ and $b_{t,k} = 0$ when $P^S_{t,k} \leq 0$, yielding $P^L_{t,k} = e^d_k P^S_{t,k}$ and $P^L_{t,k} = -e^c_k P^S_{t,k}$, according to constraints (6c) and (6d), respectively.

2) Exact Model E_2: The second exact ESS model replaces $P^S_{t,k}$ with separate variables for the charging and discharging power, $P^c_{t,k} \geq 0$ and $P^d_{t,k} \geq 0$, defined as

$$P^S_{t,k} = P^d_{t,k} - P^c_{t,k}, \quad \forall t \in \mathcal{T}, k \in \mathcal{K}. \quad (7)$$

Using (7), the power losses in (4)-(5) are reformulated as

$$P^L_{t,k} = e^d_k P^d_{t,k} + e^c_k P^c_{t,k}, \quad \forall t \in \mathcal{T}, k \in \mathcal{K}. \quad (8a)$$
$$P^d_{t,k} \perp P^c_{t,k}, \quad \forall t \in \mathcal{T}, k \in \mathcal{K}. \quad (8b)$$

The non-convex complementarity constraints (8b) ensure non-simultaneous charging and discharging, such that $P^L_{t,k} = e^d_k P^d_{t,k}$ and $P^L_{t,k} = e^c_k P^c_{t,k}$ when $P^S_{t,k} \geq 0$ and $P^S_{t,k} \leq 0$, respectively. Replacing (7)-(8a) in (1a) [4] yields the model formulation [8], for all $t \in \mathcal{T}$, $k \in \mathcal{K}$

$$C_{t+1,k} = C_{t,k} + \Delta T(-P^d_{t,k}/\eta^d_k + \eta^c_k P^c_{t,k}), \quad (9a)$$
$$0 \leq P^d_{t,k} \leq \overline{P}^d_{t,k}, \; 0 \leq P^c_{t,k} \leq \overline{P}^c_{t,k}, \quad (9b)$$
$$\text{Constraints (1b), (8b)}, \quad (9c)$$

where constants $\eta^d_k = 1/(1 + e^d_k)$ and $\eta^c_k = 1 - e^c_k$ denote the discharging and charging efficiency coefficients. The complementarity constraints (8b) can be modelled using type 1 special ordered set (SOS-1[1]) constraints, as SOS-1$(P^d_{t,k}, P^c_{t,k})$.

3) Exact Model E_3: This model reformulates the complementarity constraints (8b) using binary variables [9], yielding

$$\text{Constraints (1b), (9a)} - \text{(9b)}, \quad (10a)$$
$$P^d_{t,k} \leq (1 - b_{t,k})\overline{P}^d_{t,k}, \quad \forall t \in \mathcal{T}, k \in \mathcal{K}, \quad (10b)$$
$$P^c_{t,k} \leq b_{t,k}\overline{P}^c_{t,k}, \quad b_{t,k} \in \{0, 1\}, \quad \forall t \in \mathcal{T}, k \in \mathcal{K}. \quad (10c)$$

[1]The SOS-1 constraint involves a set of variables where at most one variable in the set can take a non-zero value (see [13], Section 9.3). In this work, SOS-1 constraints are handled automatically by the optimization solver, where these constraints are treated directly by the branch-and-cut algorithm or are reformulated using binary or integer variables [14].

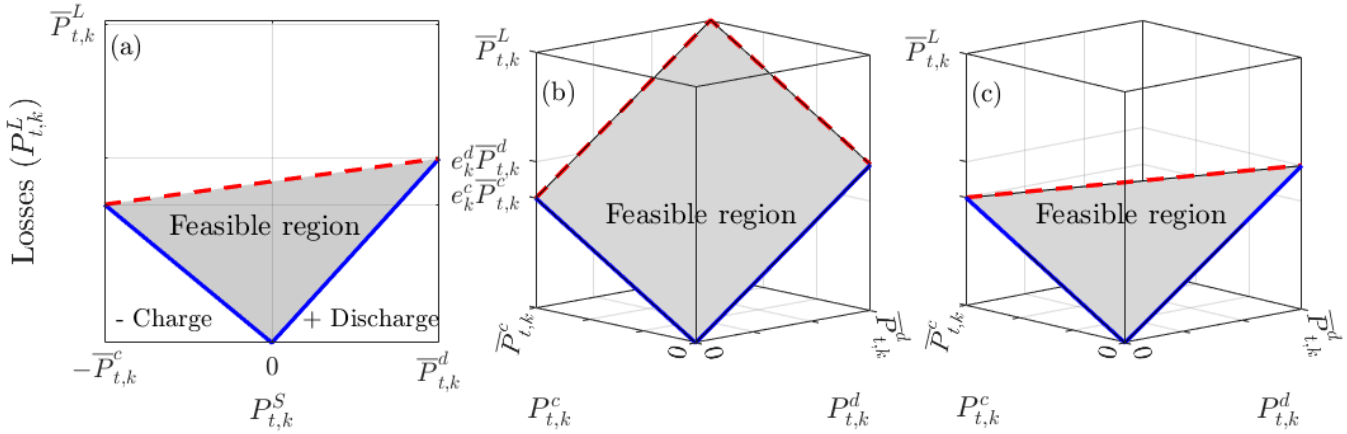

Fig. 1. Power losses of the three ESS models as a function of the charging/discharging power: (a) *Model* 1, (b) *Model* 2, and (c) *Model* 3. The blue solid lines have the dual role of indicating the feasible region of the exact models and providing lower bounds on the power losses with respect to the relaxed models. Similarly, the red dashed lines provide upper bounds on the power losses, such that the shaded areas are the feasible regions of the relaxed models.

B. Relaxed ESS Models

1) Relaxed Model R_1: Deriving the convex hull of constraint (5) [5] yields the first relaxed model as

$$\text{Constraints (1a)} - \text{(1c)} \tag{11a}$$

$$P^L_{t,k} \geq e^d_k P^S_{t,k}, \quad P^L_{t,k} \geq (-e^c_k) P^S_{t,k}, \quad \forall t \in \mathcal{T}, k \in \mathcal{K}, \tag{11b}$$

$$P^L_{t,k} \leq e^c_k \overline{P}^c_{t,k} + \alpha_{t,k}(P^S_{t,k} + \overline{P}^c_{t,k}), \quad \forall t \in \mathcal{T}, k \in \mathcal{K}, \tag{11c}$$

where constant $\alpha_{t,k} = (e^d_k \overline{P}^d_{t,k} - e^c_k \overline{P}^c_{t,k})/(\overline{P}^d_{t,k} + \overline{P}^c_{t,k})$. Affine constraints (11b) and (11c) provide lower and upper bounds on the power losses according to (5).

2) Relaxed Model R_2: Removing the complementarity constraints (8b) [7] yields the second convex model

$$\text{Constraints (1b), (9a)} - \text{(9b)}. \tag{12}$$

3) Relaxed Model R_3: Relaxing the binary variables to take continuous values in (10c) of *Model* E_3 [9], yields

$$\text{Constraints (1b), (9a)} - \text{(9b), (10b)}, \tag{13a}$$

$$P^c_{t,k} \leq b_{t,k} \overline{P}^c_{t,k}, \quad 0 \leq b_{t,k} \leq 1, \quad \forall t \in \mathcal{T}, k \in \mathcal{K}. \tag{13b}$$

C. Relaxation Exactness and Tightness

The three exact ESS models are equivalent, always generating the optimal solution, because *Models* E_2 and E_3 are reformulations of *Model* E_1. The relaxed *Model* R_1 provides the same solution with the exact models when equality is attained (active constraint) in one of the two constraints in (11b), otherwise increased power losses occur. Similarly, the relaxed *Models* R_2 and R_3 are exact when simultaneous charging and discharging do not occur.

Fig. 1 depicts the feasible region of the power losses for both the exact and relaxed versions of *Models* 1 - 3[2] as a function of the charging/discharging power. As can be observed, the relaxation of *Models* 1 and 3 is tight because the feasible region of these relaxed models (R_1 and R_3) is the convex hull of the feasible region of the corresponding exact models (E_1 and E_3). On the contrary, *Model* R_2 is not tight as illustrated in Fig. 1(b). Figs. 1(a) and 1(c) further indicate that *Models* R_1 and R_3 are equivalent in terms of power losses, since they have the same feasible region. This observation can also be verified mathematically. By replacing $P^L_{t,k}$ with (8a) and setting $P^S_{t,k} = P^d_{t,k} - P^c_{t,k}$, it can be shown that the constraints of *Model* R_1, i.e., (11a)-(11c), are the same with those of *Model* R_3, i.e., (13a)-(13b).

[2]We will jointly refer to *Models* E_i and R_i as *Model* i, where $i = \{1, 2, 3\}$.

IV. Unit Commitment

This section investigates the performance of the ESS models by incorporating them in the UC problem. The UC problem schedules the generating resources to satisfy the load demand over a planning horizon at minimum cost. In this work, we schedule the conventional generating units and ESSs to ensure the power balance between generation and demand, including ramping constraints of the generating units. Similarly with [12], ramping constraints are included in the formulation because they may cause the ESSs relaxation violation.

A. Objective function

The objective is to minimize the quadratic cost functions of the generating units, given by

$$\text{minimize} \quad \Delta T \sum_{t \in \mathcal{T}} \sum_{g \in \mathcal{G}} (\hat{\alpha}_g z_{t,g} + \hat{\beta}_g P^G_{t,g} + \hat{\gamma}_g (P^G_{t,g})^2) \tag{14}$$

where $\mathcal{G} = \{1, ..., G\}$ denotes the set with the generating units and variables $P^G_{t,g}$ and $z_{t,g} \in \{0, 1\}$ denote the generating power and *on/off* status of the generating unit $g \in \mathcal{G}$ at time $t \in \mathcal{T}$, respectively. Constants $\hat{\alpha}_g$, $\hat{\beta}_g$, and $\hat{\gamma}_g$ denote the coefficients of the cost function of the generating unit $g \in \mathcal{G}$. In objective (14), the fixed cost $\hat{\alpha}_g$ is included in the objective only when the unit is *on*, $z_{t,g} = 1$.

B. Constraints

Power limits constraints ensure the operation of the generating units between their minimum and maximum power limits ($\underline{P}^G_g, \overline{P}^G_g$) when the units are *on*, $z_{t,g} = 1$, defined as

$$z_{t,g} \underline{P}^G_g \leq P^G_{t,g} \leq z_{t,g} \overline{P}^G_g, \quad \forall t \in \mathcal{T}, \forall g \in \mathcal{G}. \tag{15}$$

According to constraint (15), $P^G_{t,g} = 0$ when $z_{t,g} = 0$.

The power balance between produced power from the conventional units, ESSs discharging and charging power, and load demand $\hat{D}_t$, is stated as

$$\sum_{g\in\mathcal{G}} P^G_{t,g} + \sum_{k\in\mathcal{K}} P^S_{t,k} = \hat{D}_t, \quad \forall t \in \mathcal{T}. \tag{16}$$

Ramp-up constraints that limit the units power increment between two consecutive time intervals are given by

$$P^G_{t,g} - P^G_{t-1,g} \leq \Delta T(R^U_g z_{t-1,g} + R^{SU}_g(z_{t,g} - z_{t-1,g})) + \overline{P}^G_g(1 - z_{t,g}), \quad t \in [2,T], \forall g \in \mathcal{G}, \tag{17}$$

where constants R^U_g and R^{SU}_g denote the generation upward and start-up ramp rates. Similarly, ramp-down constraints are set as

$$P^G_{t-1,g} - P^G_{t,g} \leq \Delta T(R^D_g z_{t,g} + R^{SD}_g(z_{t-1,g} - z_{t,g})) + \overline{P}^G_g(1 - z_{t-1,g}), \quad t \in [2,T], \forall g \in \mathcal{G}, \tag{18}$$

where constants R^D_g and R^{SD}_g denote the generation downward and shutdown ramp rates. Similarly with [12], start-up and shutdown costs, minimum up and down times and reserves are ignored because the building of the exact UC formulation is out of the scope of this work.

The considered UC problem with an integrated ESS model is summarized as

$$\mathbb{U}: \begin{cases} \text{minimize Objective (14)} \\ \text{subject to: Constraints (15)} - \text{(18)}, \textit{ESS Model.} \end{cases}$$

The following optimization formulations are derived by incorporating the presented ESS models in Problem $\mathbb{U}$:

- **Problem** $\mathbb{U}^E_i$: Uses the exact ESS model, *Model* E_i, where $i = \{1, 2, 3\}$.
- **Problem** $\mathbb{U}^R_i$: Uses the relaxed ESS model, *Model* R_i, where $i = \{1, 2, 3\}$.

Note that when *Models* 2 - 3 are used, then $P^S_{t,k}$ is replaced by $P^d_{t,k} - P^c_{t,k}$ in (16). Problem $\mathbb{U}^E_2$ is a mixed-integer quadratic program (MIQP) with SOS-1 constraints and the rest problems are MIQPs. Problems $\mathbb{U}^R_1$ - $\mathbb{U}^R_3$ have a reduced number of binary variables compared to Problems $\mathbb{U}^E_1$ - $\mathbb{U}^E_3$, expecting to result in lower execution times.

V. Simulation Results

This section investigates the performance of the ESSs models in the context of the UC problem (Problems $\mathbb{U}^E_1$, $\mathbb{U}^E_2$, $\mathbb{U}^E_3$, $\mathbb{U}^R_1$, $\mathbb{U}^R_2$, and $\mathbb{U}^R_3$). All problems are coded in Matlab and solved using optimization solver Gurobi [14], using the Matlab interface for Gurobi 9.5.2, on a personal computer with 8 GB RAM and an Intel Core-i5 3.2 GHz processor. To examine the solution quality of Problems $\mathbb{U}^R_1$, $\mathbb{U}^R_2$, and $\mathbb{U}^R_3$, which use the relaxed ESS models, the optimality gap metric is considered

$$\text{Optim. Gap} = \frac{\text{Solut. value} - \text{Optim. value}}{\text{Optim. value}} \times 100\%, \tag{19}$$

where the optimal value is obtained by solving the corresponding problems with the exact ESSs models. The following cases can be observed depending on the value of the optimality gap:

TABLE I
Units Coefficients

	$\underline{P}^G_g$	$\overline{P}^G_g$	$\hat{\alpha}_g$	$\hat{\beta}_g$	$\hat{\gamma}_g$	$R^U_g = R^D_g = R^{SU}_g = R^{SU}_g$
Unit 1:	2.4 MW	50 MW	0.5	3	0.02	15 MW
Unit 2:	2.4 MW	50 MW	5	19.9	0.04	15 MW

TABLE II
ESSs Coefficients

	$\underline{C}_k$	$\overline{C}_k$	I_k	$\overline{P}^d_k = \overline{P}^c_k$	$\eta^d_k = \eta^c_k$
ESS 1:	1.0 MWh	4.0 MWh	3.0 MWh	5.0 MW	0.89
ESS 2:	3.0 MWh	6.5 MWh	5.5 MWh	5.5 MW	0.91
ESS 3:	0.5 MWh	1.5 MWh	1.0 MWh	1.5 MW	0.88
ESS 4:	0.5 MWh	1.0 MWh	0.5 MWh	0.5 MW	0.92
ESS 5:	0.5 MWh	0.7 MWh	0.5 MWh	0.5 MW	0.89
ESS 6:	0.5 MWh	0.7 MWh	0.5 MWh	0.5 MW	0.91

TABLE III
Load Demand

t (h)	1	2	3	4	5	6	7	8	9	10	11	12
$\hat{\mathbf{D}}_\mathbf{t}$ **(MW)**	10	36	28	38	14	46.1	39	34	38	43	36	28
t (h)	13	14	15	16	17	18	19	20	21	22	23	24
$\hat{\mathbf{D}}_\mathbf{t}$ **(MW)**	38	14	49	40	28	17	14	22	29	39	49	38

TABLE IV
Case Studies

Cases	S_1	S_2	S_3	S_4	S_5	S_6	S_7
Total Units:	2	28	30	32	34	36	38
Total ESSs:	6	84	90	96	102	108	114
Load Magnitude:	$\times 1$	$\times 14$	$\times 15$	$\times 16$	$\times 17$	$\times 18$	$\times 19$

1) Optimality gap $= 0$: The optimal solution is generated if the ESSs relaxation is exact.
2) Optimality gap < 0: A lower bound solution on the optimal value is obtained, where the ESSs relaxation is non-exact and the solution is infeasible.

A. Setup

The simulation setup is composed of 2 generating units and 6 ESSs presented in Tables I and II as well as the 24 hours load demand shown in Table III, defined as case study S_1. In Table IV we consider case studies $S_1 - S_7$ with an increased number of units and ESSs by (a) duplicating the units and ESSs of study S_1 and (b) multiplying the load demand with the load magnitude of Table IV. Note that we selected the aforementioned case studies in a way to cause the violation of the ESSs relaxation exactness in Problems $\mathbb{U}^R_i$, $i = \{1, 2, 3\}$.

B. Aggregate results

Fig. 2(a) shows the increasing execution times of Problems $\mathbb{U}^E_i$ and $\mathbb{U}^R_i$, $i = \{1, 2, 3\}$, for the case studies $S_1 - S_7$. Comparing the exact models, problems U^E_2 and U^E_3 achieve similar execution times between them and better execution times compared to U^E_1. As expected, Problems $\mathbb{U}^R_i$, $i = \{1, 2, 3\}$, with the relaxed models have significantly lower execution times compared to the exact models and Problem U^R_1 has the lowest times for $S_5 - S_7$. However, the exactness of the relaxed models is violated in $U^R_1 - U^R_3$ under the selected input data, resulting in the optimality gap shown in Fig. 2(b). As expected from the analysis in Section III-C, Problem U^R_2 presents the largest negative optimality gap, while U^R_1 and

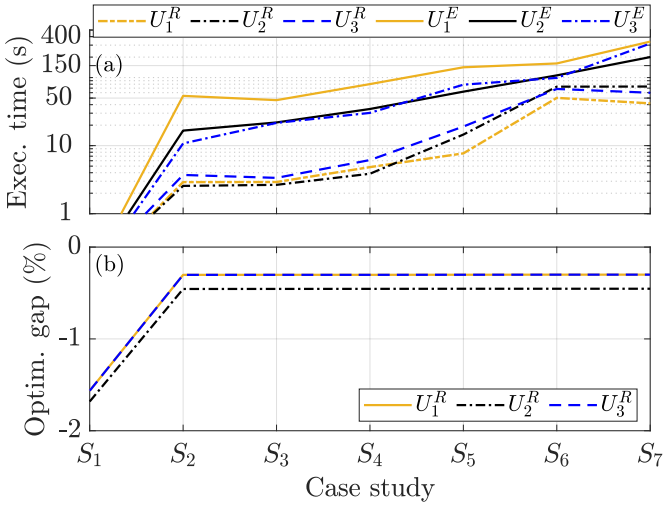

Fig. 2. Aggregate results: (a) execution time (s) and (b) optimality gap (%). The execution times of all problems for S_1 are less than 1 second.

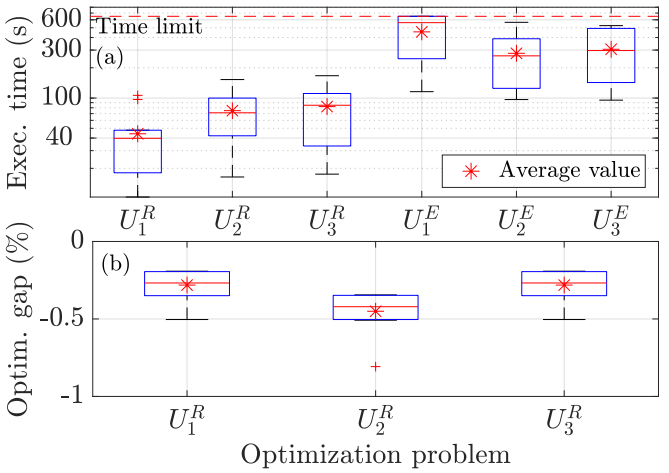

Fig. 3. Aggregate results for the case study S_7 under variations of the load demand: (a) execution time (s) and (b) optimality gap (%).

U_3^R yield the same optimality gap because Models R_1 and R_3 are tight. Note that larger negative optimality gaps correspond to higher artificial ESS power losses that cause a mismatch between the estimated and actual SoC of the real ESSs, leading to the violation of the maximum SoC limit. However, the primary controllers integrated in real ESSs ensure the SoC limits by limiting the charging/discharging power; but, this action can cause a mismatch between scheduled and actual operation of the real system.

The performance of the ESS models is further examined under case study S_7 with load demand variations. Specifically, 10 new case studies are created by adding a random value, between $[-1, 1]$, in each time interval of the load. Fig. 3(a) illustrates the execution times of the considered problems in box-plot form, where the solver time limit was set to 650 s, and Fig. 3(b) depicts the optimality gap of Problems $U_1^R - U_3^R$. Interestingly, the relaxation exactness is always violated in the selected case studies; thus, the optimality gap in Fig. 3(b) is always negative. The results indicate that Models E_2 and E_3 are preferable among the exact models because they yield the lowest execution times. In addition, Model R_1 is preferable among the relaxed models because is the fastest model and presents the lowest optimality gap, in absolute value, when the relaxation exactness is violated.

VI. Conclusions

This work examined the exact and relaxed versions of three piecewise linear ESS models, in terms of their solution quality and execution efficiency, by integrating them in the UC problem. From the obtained results, the following usage recommendations can be made. Exact Models E_1-E_3 are non-convex, generating the optimal solution but resulting in high execution times. Relaxed Models R_1-R_3 are convex and can be used (a) in applications that require fast solutions, e.g., real-time applications, by formulating convex optimization problems or (b) in mixed-integer programs to reduce their computational time. The relaxed models generate the optimal solution when the relaxation exactness holds true; otherwise, increased ESS losses occur that can cause a mismatch between scheduled and actual operation of the real system. Models E_2-E_3 and R_1 are preferable among the exact and relaxed models, respectively, because they are the fastest models and Model R_1 yields the lowest optimality gap in absolute value. Future work will investigate the impact of the relaxation violation on the actual system operation.

References

[1] IRENA, "Electricity Storage and Renewables: Costs and Markets to 2030," 2017.

[2] N. Günter et al., "Energy storage for grid services and applications: Classification, market review, metrics, and methodology for evaluation of deployment cases," in *Journal of Energy Storage*, vol. 8, pp. 226–234, 2016.

[3] European Commission, "2050 Climate and Energy Strategy".

[4] P. Haessig, "Convex Storage Loss Modeling for Optimal Energy Management," in *Proc. 2021 IEEE Madrid PowerTech*, 2021, pp. 1-6.

[5] L. Tziovani et al., "Energy Management and Control of Photovoltaic and Storage Systems in Active Distribution Grids," in *IEEE Trans. on Power Systems*, vol. 37, no. 3, pp. 1956-1968, May 2022.

[6] Q. Li, R. Ayyanar and V. Vittal, "Convex Optimization for DES Planning and Operation in Radial Distribution Systems With High Penetration of Photovoltaic Resources," in *IEEE Trans. on Sustainable Energy*, vol. 7, no. 3, pp. 985-995, July 2016

[7] R. Zafar et al., "Optimal Dispatch of Battery Energy Storage System Using Convex Relaxations in Unbalanced Distribution Grids," in *IEEE Trans. on Industrial Informatics*, vol. 16, no. 1, pp. 97-108, Jan. 2020.

[8] Z. Li et al., "Sufficient Conditions for Exact Relaxation of Complementarity Constraints for Storage-Concerned Economic Dispatch," in *IEEE Trans. on Power Systems*, vol. 31, no. 2, pp. 1653-1654, March 2016.

[9] M. F. Zia et al., "Energy Management System for an Islanded Microgrid With Convex Relaxation," in *IEEE Trans. on Industry Applications*, vol. 55, no. 6, pp. 7175-7185, Dec. 2019.

[10] K. Garifi et al., "Convex Relaxation of Grid-Connected Energy Storage System Models With Complementarity Constraints in DC OPF," in *IEEE Trans. on Smart Grid*, vol. 11, no. 5, pp. 4070-4079, Sept. 2020

[11] Y. Wen et al., "Enhanced Security-Constrained Unit Commitment With Emerging Utility-Scale Energy Storage," in *IEEE Trans. on Power Systems*, vol. 31, no. 1, pp. 652-662, Jan. 2016.

[12] J. M. Arroyo et al., "On the Use of a Convex Model for Bulk Storage in MIP-Based Power System Operation and Planning," in *IEEE Trans. on Power Systems*, vol. 35, no. 6, pp. 4964-4967, Nov. 2020.

[13] H. Paul Williams, "Model Building in Mathematical Programming," *Wiley*, 5th edition, 2013.

[14] Gurobi Optimization, LLC, "Gurobi Optimizer Reference Manual," 2022. [Online]. Available: "http://www.gurobi.com".